A 2D Differential Equations Model for Mutualism

Wendy Gruner Graves
Rainy River Community College
wgraves@rrcc.mnscu.edu

Bruce B. Peckham,
Department of Mathematics and Statistics
University of Minnesota Duluth
bpeckham@d.umn.edu

John Pastor
Department of Biology
University of Minnesota Duluth and NRRI, University of Minnesota,
jpastor@nrri.umn.edu

Department of Mathematics and Statistics
Technical Report TR 2006-2
University of Minnesota Duluth
2006

NOTE: This technical report is an expanded version of a paper by the same authors entitled “A Bifurcation Analysis of a Differential Equations Model for Mutualism.” The shorter version was accepted on August 9, 2005 and is expected to appear in the Journal of Mathematical Biology in 2006. Much of the work in both papers appeared first as part of a Masters of Science project report written by W. Graves under the direction of B. Peckham and J. Pastor (Graves 2003).

Abstract:

We develop from basic principles a two-species differential equations model which exhibits mutualistic population interactions. The model is similar in spirit to a commonly cited model (Dean 1983), but corrects problems with singularities in that model. In addition, we investigate our model in more depth. The behavior of the system is investigated by varying the intrinsic growth rate for each of the species and analyzing the resulting bifurcations in system behavior. We are especially interested in transitions between facultative and obligate mutualism. The model reduces to the familiar Lotka-Volterra model locally, but is more realistic globally in the case where mutualist interaction is strong. In particular, our model supports population thresholds necessary for survival in certain cases, but does this without allowing unbounded population growth. Experimental implications are discussed for a lichen population.

1 Introduction

Mutualism is defined as an interaction between species that is beneficial for both species. A facultative mutualist is a species that benefits from interaction with another species, but does not absolutely require the interaction, whereas an obligate mutualist is a species that cannot survive without the mutualist species. There are many interesting examples in ecology of mutualist interactions, and there exists a number of mathematical models for two-species mutualism in the literature, although the volume of work on mutualism is dwarfed by the volume of work dealing with predator-prey and competition interaction. For a review and discussion of mutualism models through the mid 1980's – still frequently referred to – see Wolin (1985).

In this paper we develop a model that can be used to describe both obligate and facultative mutualism, as well as transitions between the two. These transitions may be of interest in understanding populations whose birth rates are influenced by controllable factors such as the environment (see, for example Hernandez 1998). Transitions between different types of mutualism are also important from an evolutionary perspective.

One commonly cited reference, developed to account for both facultative and obligate mutualism, was presented in Dean (1983). To limit population growth, Dean introduced a model for two mutualistic populations where each population's carrying capacity saturated as the other population increased. Thus positive feedback between the two mutualists could not cause the solutions to grow without bound. Modeling mutualism through effects of each species on the other's carrying capacity is a common technique in mutualism models (Wolin 1985). In particular, obligate mutualists are assigned a negative carrying capacity in isolated growth whereas facultative mutualists have a positive carrying capacity in isolation, albeit a lower one than when grown in the presence of the other species.

We found Dean's model appealing, but upon examination determined that there was a problem with the derivation of the equations and therefore in applying the model to the case of obligate mutualism and therefore to the transition between facultative and obligate cases. Briefly, as carrying capacity passed through zero, a singularity in the model moved into the first quadrant of the phase space and made the interpretations incorrect when either population was obligate (see the Appendix for further explanation).

The model we present here is similar in spirit to Dean's model. We call it the "limited per capita growth rate mutualism model":

$$\begin{aligned} \frac{dx}{dt} &= (r_{10} + (r_{11} - r_{10})(1 - e^{-k_1 y}))x - a_1 x^2 \\ \frac{dy}{dt} &= (r_{20} + (r_{21} - r_{20})(1 - e^{-k_2 x}))y - a_2 y^2 \end{aligned} \qquad (1)$$

Like Dean's model, it features saturating benefits to both populations but unlike Dean's model it assumes that each mutualist asymptotically enhances the other's growth rate rather than directly affecting carrying capacity. It produces results qualitatively similar to Dean's model when both populations are facultative, but eliminates the difficulties encountered with Dean's model when either mutualist is obligate. Thus, our model can be used to describe facultative-facultative ($r_{10}>0$, $r_{20}>0$), facultative-obligate ($r_{10}>0$, $r_{20}<0$ or $r_{10}<0$, $r_{20}>0$), obligate-obligate ($r_{10}<0$, $r_{20}<0$) mutualism as well as smooth dynamical transitions that may occur between and among these types of mutualism. It may therefore

be useful in guiding further experimental studies and in the theory of the evolution of different types of mutualism.

We analyze the models in this paper using a bifurcation point of view. In our approach we identify two of our parameters as "primary" and the remaining as "auxiliary." We choose r_{10} and r_{20}, the parameters which determine the birth rates of each of our populations in the absence of the other (their signs determining facultative vs. obligate), as our primary parameters. In general, we fix a set of auxiliary parameters, compute bifurcation curves which divide the r_{10}-r_{20} parameter plane into equivalence classes, and provide representative phase portraits for each class. We then use the bifurcation diagrams and phase portraits to determine the implications for the ecology of the populations. This amounts to a courser division of the parameter space than obtained via bifurcation theory because we include only bifurcations that cause changes to the first quadrant of phase space. Finally, we attempt to classify the r_{10}-r_{20} bifurcation diagrams as the auxiliary parameters are varied. Bifurcation analysis is relatively new to ecology (see Kot 2001 for some examples), and to our knowledge has not been applied to understanding how different types of mutualism relate to one another.

The remainder of the paper is organized as follows. The limited per capita growth rate model is developed in Section 2. In Section 3, we analyze the model. It turns out that, to lowest order terms, our model reduces to the well-known Lotka-Volterra model. Thus, a byproduct of our analysis is a bifurcation analysis of the Lotka-Volterra model. In Section 4 we describe a lichen symbiosis to which our model can be applied. We also suggest possible experiments to which our model might be applied. Results are summarized in Section 5, and we point out the singularity in the original Dean model in the Appendix.

We consider the following to be new in this paper: identification of the singularity in the Dean model, the development of our limited growth rate model (although Kot (2001) presents a brief discussion of a model in which the mutualist decreases the density dependence of birth rate but has no effect on death rate of the other species), the bifurcation analysis of the limited growth rate model, including the bifurcation analysis of the Lotka-Volterra model.

2 Development of the model

We now develop our two species model with the following assumptions:

- A1: The logistic assumption: Each species behaves according to the logistic model.
- A2: The growth rate assumption: Each species affects the other species' per capita growth rate, but not its self limitation.
- A3: The mutualism assumption: The increase in each species cannot harm the other species.
- A4: The limited benefit assumption: There is a maximum per capita growth rate attainable for each species.
- A5: The proportional benefit assumption: The marginal rate of change of the per capita growth rate of each species due to the increase of the other species is proportional to the difference between the maximum growth rate and the current growth rate.

Assumptions A1 and A2 lead to the following general form:

$$\frac{dx}{dt} = R_1(y)x - a_1x^2$$
$$\frac{dy}{dt} = R_2(x)y - a_2y^2 \qquad (2)$$

Assumption A3 can be stated mathematically as $R_1'(y) \geq 0$ and $R_2'(x) \geq 0$. Assumption A4 can be stated mathematically as the existence of maximum growth rates r_{11} for species x, and r_{21} for species y, satisfying $R_1(y) \leq r_{11}$ and $R_2(x) \leq r_{21}$. Assumption A5 can be restated as $R_1'(y)=k_1(r_{11} - R_1(y))$ and $R_2'(x)=k_2(r_{21} - R_2(x))$. These two linear differential equations can be easily solved to obtain

$$R_1(y) = r_{10} + (r_{11} - r_{10})(1 - e^{-k_1y})$$
$$R_2(x) = r_{20} + (r_{21} - r_{20})(1 - e^{-k_2x}) \qquad (3)$$

where the parameters r_{10} and r_{20} are the respective unaided growth rates of each species: $r_{10}=R_1(0)$, and $r_{20}=R_2(0)$. The combination of equations (2) and (3) above leads to the form of the main model studied in this paper: the limited per capita growth rate mutualism. This system was already stated in the introduction:

$$\frac{dx}{dt} = (r_{10} + (r_{11} - r_{10})(1 - e^{-k_1y}))x - a_1x^2$$
$$\frac{dy}{dt} = (r_{20} + (r_{21} - r_{20})(1 - e^{-k_2x}))y - a_2y^2 \qquad (1)$$

Assumption A1 requires $a_1>0$ and $a_2>0$; assumption A3 requires $r_{10} \leq r_{11}$ and $r_{20} \leq r_{21}$; assumption A5 requires $k_1>0$ and $k_2>0$. Note that for species x (y) to have any chance of survival, it must be true that $r_{11} > 0$ ($r_{21} > 0$).

Discussion: The development of our model parallels the development in Dean (1983) with the significant difference that we saturate the per capita growth rate instead of the carrying capacity. An alternative model could have been developed assuming that the mutualism was effected through the quadratic term instead of or in addition to the per capita growth rate term, but we chose to stay with the growth rate term because it seemed to fit the population interaction we had in mind. In addition, the resulting model exhibited both key behaviors we expected from realistic mutualist populations: bounded population growth and the existence of threshold population values below which populations die out and above which populations persist.

Parameter (non)reduction. A common mathematical technique at this point is to rescale both the x and y variables to eliminate (that is, "make equal to one") parameters a_1 and a_2. We choose not to make this parameter reduction in order to retain the original interpretation of the parameters.

3. Analysis of the model

In this section we perform a bifurcation analysis of the limited per capita growth rate mutualism model in equation (1). For fixed values of the auxiliary parameters our general goal is to divide the r_{10}-r_{20} parameter plane into "equivalence classes," where two differential equations are defined to be equivalent if their "phase portraits" are

qualitatively the same. (The formal equivalence is called "topological equivalence." See, for example, Guckenheimer and Holmes (1983), Strogatz (1994), Robinson (2004)).

We display our results via a bifurcation diagram in the r_{10}-r_{20} parameter plane that illustrates the equivalence classes, and accompanying phase portraits in the x-y plane, one for each equivalence class, which illustrate the corresponding dynamics. The phase portraits include the following: nullclines (dashed lines), equilibria (at the intersections of nullclines), accompanying equilibria labels (according to the tables in sections 3.2 and 3.3), stability of the equilibria (filled circle for attracting, open circle for repelling, half circle for saddle), and the stable and unstable manifolds of any saddles; arrows on the two branches of the unstable manifold (the two distinguished orbits which approach the saddle equilibrium point in backward time) point away from the saddle equilibrium point, while arrows on the two branches of the stable manifold (the two distinguished orbits which approach the saddle equilibrium point in forward time) point toward the saddle equilibrium point.

Because the Poincare-Bendixon theorem (see for example Guckenheimer and Holmes 1983, Hirsch, et. al. 2004, Strogatz 1994, Robinson 2004) guarantees that, for two-dimensional differential equations, orbits that stay away from equilibrium points must either be, or limit to, a periodic orbit, we include periodic orbits when they exist. We note that periodic orbits are impossible in the first quadrant of phase space for mutualism models in the general form of equation (2) and satisfying assumptions A1, A2, and A3 in Section 2. This result can be proved geometrically by contradiction: if there were a periodic orbit, the conditions on the dx/dt equation would allow only a clockwise flow, while the conditions on the dy/dt equation would allow only a counterclockwise flow (It can also be proved algebraically that equilibria cannot have complex eigenvalues by showing that the discriminant of the Jacobian derivative is always positive in the first quadrant of phase space. This precludes the possibility of the birth of a periodic orbit through a Hopf bifurcation.)

We divide the analysis of our model into two steps: local and global. It turns out that locally (in variables x, y, r_{10}, r_{20}) our model reduces to the familiar Lotka-Volterra model of mutualism, so we treat the Lotka-Volterra case first. (A similar approximation is mentioned by Goh (1979) for the phase variables x and y only.) There are two subcases to consider: weak mutualism and strong mutualism. Then we consider the full model. In each of the two steps of our analysis, we first investigate only the equilibria and their bifurcations. Subsequently we consider the full bifurcation diagrams. Some bifurcation curves are determined analytically, while others are numerically followed using the dynamical systems software *To Be Continued …* (Peckham, 1986-2006). Finally we use the bifurcation diagrams to identify transitions which affect the first quadrant of the phase space, and are therefore "ecologically significant."

The bifurcation curves we encounter in this study are all standard "codimension-one bifurcations" in dynamical systems theory: transcritical (the crossing of a solution with either $x \equiv 0$ or $y \equiv 0$ by another solution)), saddle-node (the birth of a pair of equilibrium points), Hopf (the change in stability of an equilibrium point with complex eigenvalues, accompanied by the birth of a limit cycle), homoclinic (the crossing of a branch of the stable manifold of a saddle equilibrium point with a branch of the unstable manifold of the same point) and heteroclinic (the crossing of a branch of the stable manifold of a saddle equilibrium point with a branch of the unstable manifold of a different saddle

equilibrium point). See introductory dynamical systems texts (Guckenheimer and Holmes 1983, Strogatz 1994, Hirsch et. al. 2004, Robinson 2004) for further explanation.

3.1 Local reduction to the Lotka-Volterra model

By expanding the exponential terms in equation (1) in a Taylor series, one can rewrite the limited growth rate model - up through quadratic terms *in the phase variables and the primary parameters together* - as:

$$\begin{aligned} \frac{dx}{dt} &= (r_{10} + k_1 r_{11} y)x - a_1 x^2 + O(xy^2, r_{10}xy) \\ \frac{dy}{dt} &= (r_{20} + k_2 r_{21} x)y - a_2 y^2 + O(x^2 y, r_{20}xy) \end{aligned} \tag{4}$$

The "big-Oh" terms are higher order terms. Thus, at least for values of x, y, r_{10}, and r_{20} close to zero, the dynamics of our limited growth rate model should match that of the Lotka-Volterra interaction model:

$$\begin{aligned} \frac{dx}{dt} &= (r_{10} + b_1 y)x - a_1 x^2 \\ \frac{dy}{dt} &= (r_{20} + b_2 x)y - a_2 y^2 \end{aligned} \tag{5}$$

with parameters r_{10}, r_{20}, a_1, a_2, b_1, b_2 in the Lotka-Volterra model corresponding to parameter combinations r_{10}, r_{20}, a_1, a_2, $k_1 r_{11}$, $k_2 r_{21}$, respectively.

Note that the Lotka-Volterra model could have been derived on its own using assumptions A1-A3 in Section 2, but replacing assumptions A4 and A5 with the assumption that the change in the per capita birth rate of each species depends linearly on the other. This results in the same general form of equation (4), but with $R_1(y)=r_{10} + b_1 y$ and $R_2(x)=r_{20}+ b_2 x$. Assumption A4 no longer holds since neither population's growth rate is bounded. Because of our assumptions on the coefficients in equation (1), b_1 and b_2 are assumed to be nonnegative, and a_1 and a_2 are assumed to be positive.

3.2 Local analysis: Lotka-Volterra interaction

Since the analysis of the Lotka-Volterra equations will determine the local dynamics for our model, we begin by analyzing equation (5). Certain aspects of this analysis have been well-known for a long time (see, for example, Vandermeer and Boucher1978, Goh, 1979, Wolin 1985, Kot 2001), but the bifurcation diagrams we present here appear to be less widely known. For this reason, and for completeness with respect to our model, we begin with the Lotka-Volterra analysis.

Equilibria. Each nullcline, $dx/dt=0$ or $dy/dt=0$, is easily seen to be one of the axes and an additional straight line. By solving simultaneously, one can find the four equilibria of this system. They are listed along with their eigenvalues in table 1. Equilibria 0, 1 and 2 are trivial cases representing survival of at most one population. Equilibrium 3 is the coexistence equilibrium. The corresponding entries for the Jacobian evaluated at this equilibrium are complicated expressions. We do not explicitly include the Jacobian or the corresponding eigenvalue expressions here.

Bifurcation analysis. It is well-known (Vandermeer and Boucher 1978; but see also Goh 1979) that this 2-D system has a stable and feasible coexistence equilibrium only when

$$a_1 a_2 > b_1 b_2 \qquad (6)$$

which corresponds to requiring that the product of the self-limiting coefficients be larger than the product of the coefficients that confer inter-specific benefit. We call the case when inequality (6) is satisfied *weak mutualism*. The opposite inequality we call *strong mutualism*. Fig. 1 shows the b_2 vs. b_1 plane (a different parameter plane from all others in this paper!) and the different kinds of interactions between the two species. The coefficients a_1 and a_2 of the self-limitation terms are assumed to be fixed positive constants. The curve that divides the first quadrant into strong versus weak mutualism is determined by setting $a_1 a_2 = b_1 b_2$. The area below the curve in the first quadrant is the region of b_2 vs. b_1 parameter space that would give rise to weak mutualism (with bounded populations), whereas the area above the curve is the area of the parameter plane that yields strong mutualism (with unbounded populations). Interestingly, the curve $a_1 a_2 = b_1 b_2$ also appears in the third quadrant where it divides the cases of weak competition (that need *not* exhibit competitive exclusion) from strong competition (that *must* exhibit competitive exclusion).

In the following two subsections we display and explain the r_{10}-r_{20} bifurcation diagram for each of the two cases: weak and strong mutualism. It turns out that the bifurcation diagrams are required to be relatively simple as guaranteed by the following lemma.

Lemma: The r_{10}-r_{20} bifurcation diagrams for the Lotka-Volterra population models are all straight line rays from the origin. (Aside: this lemma is true for competition and predator prey models as well as for mutualism.)

The lemma can be proved by showing that any differential equation on a ray in the parameter plane can be converted into any other differential equation on the ray by rescaling the two phase variables and time. Two systems being related by a change of variables implies that the two systems are equivalent. See introductory dynamical systems texts such as Strogatz (1994) or Hirsh-Smale-Devaney (2004).) An interesting further consequence of this rescaling is that the phase portrait on the "negative" of a ray can be obtained by reflecting the phase space about the x and y axes, and reversing the direction of the time flow arrows.

3.2.1 Lotka-Volterra weak mutualism case: $a_1 a_2 > b_1 b_2$, self-limitation dominates.

The dynamics of the weak mutualism case is summarized in the r_{10}-r_{20} bifurcation diagram in Fig. 2 and the accompanying phase portraits. In Fig. 2i, the nullclines have tilted from horizontal and vertical – where they would have been if there had been no mutualism ($b_1=b_2=0$) - to oblique. The coexistence equilibrium occurs at the intersection of the two oblique nullclines. This results in coexistence population values which are greater for each species than the respective carrying capacity for each species in the absence of the other.

The four transcritical bifurcation curves can easily be found analytically by computing the Jacobian matrix, evaluating it at one of the equilibrium points, and setting the determinant equal to zero. The only computational "trick" we use is to evaluate the

Jacobian with the "easier" equilibrium point when two equilibria interact. For example, in computing the 0-2 transcritical bifurcation curve, we evaluate with equilibrium 0. More significantly, for bifurcations involving equilibrium 3 (the coexistence equilibrium), we use equilibrium 2 or 1, whichever is involved in the bifurcation. This allows us to avoid using the unwieldy expressions for equilibrium 3. The resulting transcritical bifurcation formulas, with the corresponding equilibrium labels in parentheses, are: $r_{10} = 0$ (0-1), $r_{20} = 0$ (0-2), $r_{20} = -(b_2/a_1)\, r_{10}$ (1-3), $r_{20} = -(a_2/b_1)\, r_{10}$ (2-3).

Lotka-Volterra weak mutualism population behavior summary. The bifurcation curves in Fig. 2 which are "ecologically significant" are the ones which effect changes in the first quadrant of the x-y space. This results in four broad classes, separated in the bifurcation diagram by the thicker bifurcation curves.

1. Stable coexistence occurs in regions i, ii, and ii';
2. a stable x-monoculture occurs in regions iii, iv;
3. a stable y-monoculture occurs in regions iii', iv';
4. both populations become extinct in region v.

Note especially that in regions ii and ii' the stable coexistence occurs even though one of the populations is an obligate mutualist. One could argue that cases ii and ii' are ecologically different from case i, but we choose to combine them due to their similar behavior in the *open* first quadrant [compare with Fig. 1 in Vandermeer and Boucher (1979) where they list four subcases for weak (called "stable" in their paper) Lotka-Volterra mutualism]. Their four cases S1-S4 correspond to our cases i, v, ii, and iv, respectively. They do not, however, provide a parameter space bifurcation diagram organizing the cases.

3.2.2 Lotka-Volterra strong mutualism case: $a_1 a_2 < b_1 b_2$, mutualism dominates.

The dynamics of the strong mutualism case is summarized in the r_{10}-r_{20} bifurcation diagram in Fig. 3. We first look at how the phase portrait in the first quadrant of the r_{10}-r_{20} bifurcation diagram arises by starting from the corresponding phase portrait in the weak mutualism case and allowing the coefficients b_1 and b_2 to increase. One way to visualize this transition is via the evolution of the nullclines. Consider, for example, Fig. 2i. The $dx/dt = 0$ nullcline always passes through equilibrium 1 but its slope decreases as b_1 increases. In contrast, the $dy/dt = 0$ nullcline always passes through equilibrium 2, but its slope increases as b_2 increases. Consequently, as either or both of b_1 and b_2 increase, the attracting coexistence equilibrium location goes off to infinity in the first quadrant of the phase space. When $a_1 a_2 = b_1 b_2$, the two nullclines are parallel, and the coexistence equilibrium has "gone off to infinity." This is the transition between bounded and unbounded population behavior in this model.

As b_1 and b_2 continue to grow, the nullclines intersect again, but now in the third quadrant. This leaves us with the phase portrait in Fig. 3i. We will now follow a circle in the r_{10}-r_{20} parameter space of Fig. 3 to understand the rest of the transitions for this strong mutualism case. The four transcritical bifurcations are similar to the weak mutualism case: 0-2 bifurcation from i to ii, 2-3 bifurcation from ii to iii_a, 1-3 bifurcation from iv_b to v, and the 0-1 bifurcation from v to vi.

The transitions between iii_a and iv_b in the fourth quadrant of the parameter space are quite different from the weak mutualism case. In some sense they are not so relevant to

the ecology of the system since the dynamics in the first quadrant of phase space is unaffected in this sequence of transitions. On the other hand, the transitions involving other quadrants of phase space are important in order to "set up" the first quadrant changes. And they are certainly of interest from a dynamical systems point of view. The transition from iii_a (not shown) to iii_b is a change from real eigenvalues to complex eigenvalues for equilibrium 3. The borderline case is a pair of equal (real) eigenvalues. These two cases are labeled as iii_a and iii_b because either can be obtained from the other via a change of variables. Thus they are formally equivalent. On the other hand, from a visual perspective, spiraling toward the equilibrium (when it has complex eigenvalues) is different from approaching tangent to a straight line (when the equilibrium has real eigenvalues).

The transition from iii_b to iv_a is actually a double bifurcation curve: a "Hopf" curve and a heteroclinic curve. On the bifurcation curve the eigenvalues of equilibrium 3 are pure imaginary *and* there is a *heteroclinic* connection from equilibrium 1 to equilibrium 2. As the parameters are varied from region iii_b to region iv_a equilibrium 3 changes from repelling to attracting. (This is not a true Hopf bifurcation because there is no birth of a limit cycle.) Simultaneously, there is a crossing of the right hand branch of the stable manifold of equilibrium 2 with the left hand branch of the unstable manifold of equilibrium 1. At the transition point, the two branches coincide, creating the heteroclinic connection. The coincidence of the two bifurcation curves is not typical of nonlinear models. It is present because of the truncation of the differential equation at the quadratic terms, and it separates into two distinct curves – a heteroclinc curve and an actual Hopf curve – in the bifurcation diagram for the full model.

We again have an equal eigenvalue transition for equilibrium 3 between iv_a and iv_b (not shown). This leaves the eigenvalues of equilibrium 3 real in preparation for the 2-3 transcritical bifurcation between iv_b and v.

The formulas for the transcritical curves are the same as in the weak mutualism case. The other bifurcation curves were numerically continued using the software *TBC (1986-2006).*

Lotka-Volterra strong mutualism population behavior summary. All phase portraits in this strong mutualism case have orbits in the first quadrant for which both populations grow without bound. No region exhibits a stable *feasible* (open first quadrant) coexistence equilibrium. There are four distinct regions of behavior:

1. in regions i, ii, ii', iii, iii', iv, and iv', all orbits in the open first quadrant are unbounded;
2. in region v, there is a threshold curve (the stable manifold of equilibrium 3, which is a saddle) which separates first quadrant initial conditions which have unbounded orbits from those that approach an x-monoculture (and are therefore bounded). Orbits exactly on the stable manifold of equilibrium 3, of course, approach equilibrium 3;
3. similarly, in region v', the threshold curve separates unbounded orbits from those for which populations approach a y-monoculture;
4. in region vi, the threshold curve separates unbounded orbits from those for which both populations die out.

Compare these results with Fig. 1 in Vandermeer and Boucher (1979), this time with the four cases for strong (called "unstable" in their paper) Lotka-Volterra

mutualism. Their four cases U1-U4 correspond to our cases i, vi, ii, and v, respectively. Again, they do not provide a parameter space bifurcation diagram organizing the cases.

Lotka-Volterra summary. In summary, the logistic model with Lotka-Volterra interaction terms allows either stable coexistence or threshold behavior, but not both for the same parameter values. This drawback is eliminated in the limited growth rate model of the next section.

3.3 Analysis of the full limited per capita growth rate model

We now analyze our limited growth rate model of eq. (1), repeated below for ease of reference.

$$\begin{aligned} \frac{dx}{dt} &= (r_{10} + (r_{11} - r_{10})(1 - e^{-k_1 y}))x - a_1 x^2 \\ \frac{dy}{dt} &= (r_{20} + (r_{21} - r_{20})(1 - e^{-k_2 y}))y - a_2 y^2 \end{aligned} \tag{1}$$

Equilibria. Solving first for the $\frac{dx}{dt} = 0$ nullclines, we obtain $x = 0$ and

$$x = \frac{r_{10} + (r_{11} - r_{10})(1 - e^{-k_1 y})}{a_1}. \tag{7}$$

Similarly, $\frac{dy}{dt} = 0$ occurs along $y = 0$ and

$$y = \frac{r_{20} + (r_{21} - r_{20})(1 - e^{-k_2 x})}{a_2}. \tag{8}$$

Considering all four nullclines, there are possibilities for three to five equilibria, counting multiplicity, depending on the eight parameter values. We summarize in table 2.

Equilibrium 0 is the trivial solution. Equilibria 1 and 2 are monoculture solutions. Equilibria 3 and 4 are coexistence solutions resulting from the intersection of the two nonlinear nullclines of equations (7) and (8). Since both nonlinear nullclines have asymptotes, all equilibria are confined to exist to the left of the line $x = \frac{r_{11}}{a_1}$ and below the line $y = \frac{r_{21}}{a_2}$.

Furthermore, it can be seen from equations (7) and (8) that when r_{10} and/or r_{20} are sufficiently negative, the two nonlinear isoclines will not intersect; for these parameter combinations, equilibria 3 and 4 will not exist. Note also that several pairs of these equilibria could coincide; coincidence typically happens at a transcritical bifurcation, or a saddle-node bifurcation, or a further degenerate bifurcation. For example, if both $r_{10}=0$ and $r_{20}=0$, then equilibria 0, 1, 2, and either 3 or 4 (or both, in the special case where the two nonlinear equilibria are tangent) coincide.

Bifurcation Analysis: We follow the lead of the analysis of the Lotka-Volterra equations in the previous subsection and separate our model into two primary classes: locally weak mutualism and locally strong mutualism. The two cases are determined by

the auxiliary parameters. It turns out that the division of the auxiliary parameter space into two classes for the limited growth rate model is too coarse, but we will proceed in the interest of focusing on the main features. Some clarification is provided at the end of the section.

Recall from the derivation of the model in Section 2 that $r_{10} \leq r_{11}$ and $r_{20} \leq r_{21}$, so only the "quadrant" of the r_{10} - r_{20} parameter plane determined by these inequalities is relevant for our mutualism model.

3.3.1 Full model locally weak mutualism case: $a_1 a_2 > k_1 r_{11} k_2 r_{21}$, self-limitation dominates.

This case (Fig. 4) should be compared to the weak mutualism case of the Lotka-Volterra model (Fig. 2). The locally weak mutualism inequality guarantees that when $r_{10}=0$ and $r_{20}=0$, the $dy/dt=0$ nullcline passes through the origin in the x-y plane with a shallower slope than the $dx/dt=0$ nullcline. This matches the weak mutualism case for the Lotka-Volterra interaction. Because of the shape of nonlinear nullclines, this forces the two nonlinear nullclines to intersect a second time in the third quadrant. The bifurcation scenario near the origin in the r_{10}-r_{20} plane is also analogous to the weak Lotka-Volterra bifurcation scenario in the r_{10}-r_{20} plane. The labels of the bifurcations are adjusted because they involve equilibrium 4, instead of the equilibrium labeled 3 in the Lotka-Volterra analysis. Thus, the 2-4 transcritical bifurcation curve passes through the origin in the r_{10}-r_{20} bifurcation diagram of Fig. 4 with a steeper negative slope than the slope of the 1-4 transcritical bifurcation curve.

Away from the origin in the r_{10}-r_{20} plane, we see a new feature: the *saddle-node* bifurcation curve. Equilibria 3 and 4, which exist for parameter values above this curve, coincide along the curve, and cease to exist below the curve. This transition is illustrated in the corresponding adjacent phase portraits (for example v to viii, and iv or vi to vii). We do not dwell on the details of this bifurcation since the relevant dynamical transitions do not affect the first quadrant of the phase space.

Full model locally weak mutualism population behavior summary.

The first quadrant population behavior for the limited growth rate model is analogous to that for the weak mutualism Lotka-Volterra model: the parameter space is divided into four regions corresponding to

1. stable coexistence in regions i, ii, ii';
2. a stable x-monoculture in regions iii, iv, vi, vii;
3. a stable y-monoculture in regions iii', iv', vi', vii';
4. extinction in regions v and viii.

3.3.2 Full model locally strong mutualism case: $a_1 a_2 < k_1 r_{11} k_2 r_{21}$. Mutualism coefficients dominate.

The locally strong mutualism inequality now guarantees that when $r_{10}=0$ and $r_{20}=0$, the $dy/dt=0$ nullcline passes through the origin in the x-y plane with a *steeper* slope than the $dx/dt=0$ nullcline. This matches the strong mutualism case for the Lotka-Volterra interaction. But because of the shape of nonlinear nullclines, this forces the two nonlinear nullclines to intersect a second time in the *first* quadrant, resulting in a stable coexistence equilibrium, unlike the case for strong mutualism in the Lotka-Volterra model in which stable coexistence was not possible. With the exception of the coincident

"Hopf/heteroclinic" bifurcation curve of Fig. 3A, the bifurcation scenario near the origin in the r_{10}-r_{20} plane of Fig. 5A is exactly analogous. The labels on the bifurcating equilibria are even the same. Thus, the 1-3 transcritical bifurcation curve passes through the origin in the r_{10}-r_{20} bifurcation diagram of Fig. 5A with a steeper negative slope than the slope of the 2-3 transcritical bifurcation curve. The Hopf and heteroclinic bifurcation curves are now distinct (but appear to be tangent at the origin, consistent with their coincidence in Fig. 3A), allowing for the existence of a limit cycle (in the fourth quadrant) for parameter values in between them.

Away from the origin in the r_{10}-r_{20} plane, we have several new features that differ from the strong mutualism Lotka-Volterra bifurcations. One key feature (which we have already seen in the locally weak mutualism case) is the saddle-node bifurcation curve. Equilibria 3 and 4, which exist for parameter values above the saddle-node curve, come together on the curve, and cease to exist below the curve. This transition is illustrated in the corresponding adjacent phase portraits (for example vii to viii and vi to ix). There are several other bifurcations in Fig. 5A that are significant and interesting from a bifurcation point of view, but not so significant from an ecological point of view. Some of these bifurcations curves are outside the range of parameters plotted in Fig. 5A. As mentioned in the Lotka-Volterra case, these "insignificant" bifurcations *are* necessary in order to set up the "significant" bifurcations. So we let the phase portraits in Fig. 5B speak for these transitions.

For completeness and clarification, we include several additional views of the bifurcation diagram of Fig. 5A and the corresponding Fig. 5B phase portraits. Specifically, we include a schematic of Fig. 5A which is complete in the full r_{10}-r_{20} parameter space, and schematics for Fig. 5B which also include nullclines as dashed lines. Additional numerically computed (Peckham 1986-2006) versions with two enlargements follow as well for comparison with the other versions of Fig. 5A.

Full model locally strong mutualism population behavior summary.

Although the bifurcation analysis near the origin matches that of the strong mutualism Lotka-Volterra model, the full dynamical behavior does not. This is because of the existence of the attracting equilibrium number 4 away from the origin in the phase space when the parameters r_{10} and r_{20} are both zero. Thus unbounded population growth from the Lotka-Volterra model is replaced by an approach to a stable coexistence equilibrium. More significantly, we now have regions of parameter space (regions vi, vi', vii) which allow behavior not seen in the Lotka-Volterra model: the existence of thresholds between stable coexistence and extinction of one or both of the species. There are seven distinct regions in Fig. 5a.

1. in regions i, ii, iii, iv, v, ii', iii', iv', and v' all open first quadrant initial populations eventually approach a stable coexistence equilibrium;
2. in region vi, there is a threshold (the stable manifold of equilibrium 3) between a stable *x*-monoculture and the stable coexistence equilibrium;
3. in region vi' there is a similar threshold between a stable *y*-monoculture and the stable coexistence equilibrium.
4. in all other regions of the fourth quadrant, all first quadrant orbits approach the *x*-monoculture equilibrium;

5. similarly, in all other regions of the second quadrant, all first quadrant orbits approach the y-monoculture equilibrium;
6. in region vii, there is a threshold between orbits which approach the extinction of both species and the stable coexistence of both species;
7. in region viii, both populations become extinct.

Further bifurcation discussion.

Our strategy of dividing parameters into primary and auxiliary has a more formal interpretation: we are studying bifurcations (in the auxiliary parameter space) of bifurcation diagrams (in the primary r_{10}-r_{20} parameter plane). Two points in the auxiliary parameter space are defined to be equivalent if their corresponding bifurcation diagrams in the primary parameters "look the same." "Look the same" is made formal by the existence of a homeomorphism of primary parameter planes that map corresponding bifurcation curves in one primary parameter plane to bifurcation curves of the same type in the other primary parameter plane.

Our local analysis guarantees that the primary parameter plane bifurcation diagrams for our limited growth rate model must be divided into at least two equivalence classes: auxiliary parameters that correspond to locally weak versus locally strong mutualism. It turns out that there are further subdivisions of the auxiliary parameter space when we consider the global r_{10}-r_{20} parameter space. For example, we found an example of a locally weak mutualism set of auxiliary parameter values (r_{11}=20, r_{21}=2, k_1=0.5, k_2=0.25, a_1=1, a_2=1) for which the two transcritical curves cross two times (instead of not intersecting as in in Fig. 4) in the fourth quadrant. Thus it is not true that all locally weak bifurcation diagrams are equivalent. On the other hand, the senior author proved in her M.S. thesis that locally weak mutualism (the first inequality in the statement of the Theorem below) along with an additional condition (the second inequality) will guaranty that the two transcritical curves will not cross in the fourth quadrant, suggesting that a large class of locally weak mutualism models have r_{10}-r_{20} bifurcation diagrams which might *be* equivalent:

Theorem (Graves 2003)**:** *If* $\frac{a_1 a_2}{r_{21} r_{11} k_1 k_2} > 1$, *and if* $\frac{a_1}{r_{11} k_2} \geq 1$, *the transcritical bifurcation curves displayed in Fig. 4 will not intersect in the fourth quadrant.*

In the locally strong mutualism case, although it is clear that the two transcritical curves in the fourth quadrant of Fig. 5 must cross at least once, as they do for our choice of auxiliary parameters, we have not analytically checked to see whether other numbers of crossings are possible. In other words, we do not know whether the locally strong auxiliary parameters are all in the same equivalence class. In this sense, our bifurcation study is incomplete. On the other hand we have established the existence of a model exhibiting the ecological features we were seeking, including the boundedness of all orbits and the existence of threshold behavior for sufficiently strong mutualism.

4. Experimental Implications

The basic assumption of our model which distinguishes it from other models of mutualism is that each of the mutualists asymptotically increases the other's growth rate. This allows a smooth transition between facultative and obligate mutualisms without singularities, in contrast to the case in the Dean (1983) model in which each species asymptotically increased the other's carrying capacity rather than increase the other's growth rate.

There is considerable evidence that at least some important symbioses operate through asymptotic increases in growth rates rather than in carrying capacities. Some of the most-studied such cases are nitrogen-fixation symbioses between higher plants and a nitrogen-fixing microorganism such as *Rhizobium* (with soybean) or *Frankia* (with alder). It has long been known that rates of photosynthesis in the plant increase asymptotically with increased abundance of the nitrogen-fixing microorganism and that nitrogen fixation rates in the microorganism are in turn strongly controlled by supply of photosynthate from the plant. Nitrogen fixation rates in the symbiotic microorganism are strongly controlled by supply of photosynthate because the energetic cost of nitrogen fixation enzyme systems is high and carbohydrate reductants are required in the N-fixing reactions (Nutman 1976).This suggests that mutualism in nitrogen-fixing symbioses operates by each participant increasing the other's growth rate (the asumption of our model) rather than increasing the other's carrying capacity (the assumption of the Dean (1983) model and others).

A particularly interesting class of systems with nitrogen-fixing symbiosis are lichens, with a nitrogen-fixing cyanobacteria in symbiotic association with a fungus. These symbioses are especially relevant to our model since they can be facultative - facultative, facultative-obligate, and obligate-obligate associations. Lichens of the genus *Peltigera* may be an especially good model system for experimental investigation of our model because they grow relatively fast (Ahmadjian 1967). The *Peltigera* fungus is obligate whereas the N-fixing cyanobacteria (usually *Nostoc*, but also *Gloeocapsa*, and *Chroococcidiopsis*; Stewart 1980; Büdel 1992; Pandey et al. 2000) are usually facultative and can be separated from the fungus to form free living colonies. When environmental nitrogen supply is low, less than 10% of free-living *Nostoc* form specialized cells known as heterocycts in which N-fixation takes place. However, when in association with *Peltigera* fungus, these cyanobacteria are sequestered in specialized cephalopods and greater than 20% of them form heterocycts. The rate of N-fixation in lichenized *Nostoc* increases in proportion to rate of formation of heterocycts (see review by Rai 1988), suggesting that the *Peltigera* fungus increases growth rate and metabolism of the *Nostoc* symbiont compared with free-living *Nostoc*. In some species of *Peltigera* fungus, greater than 90% of the fixed atmospheric N ends up not in the *Nostoc* but in the fungus, where it is used in protein synthesis (Rai 1988). Thus, available data indicates that the symbiosis between *Peltigera* and *Nostoc* operates by each mutualist increasing growth rates and metabolism of the other, which supports the major assumption of our model.

In addition, new molecular methods offer promise in further quantifying the effect of *Peltigera* and *Nostoc* on each other's growth rates. Sterner and Elser (2002) have presented strong evidence that growth rate in many algae and other species is correlated with ribosomal RNA content, ribosomes being the site of protein synthesis. Both rDNA

and ribosomal RNA markers have recently been identified for both *Peltigera* fungus and the algal *Nostoc* symbiont (Miadlikowska and Lutzoni 2003, Miadlikowska et al. 2004). Isolation and quantification of RNA markers of *Nostoc* and of *Peltigera* could provide indices of their growth rates. Positive and asymptotic correlations of these growth rates with each other and also with independent measurements of N-fixation by the *Nostoc* would be a strong test of the basic assumption of our model and also a way to parameterize Eq. 1.

5 Summary and Discussion

In addition to the development of our limited per capita growth rate mutualism model, we are clearly advocating in this paper the bifurcation approach to analysis of ecological models. We feel this approach is useful for analyzing models, for inferring physical/ecological behavior, and for designing experiments. For example, Fig. 5A concisely summarizes as labeled in the figure, the pairings of initial per capita growth rates that allow for stable `coexistence' of mutualist pairs. As an example of ecological inference, we note that the bifurcation diagram of Fig. 5a suggests that facultative-obligate mutualism coexistence might be fairly abundant in nature. This conclusion is supported by noting the fairly large part of the fourth quadrant of primary parameter space corresponding to coexistence. On the other hand, the region of the 3rd quadrant allowing coexistence is tiny compared to the rest of the 3rd quadrant, suggesting that obligate-obligate mutualisms might be rare in nature. Of course, Fig. 5a is for one specific choice of auxiliary parameters, but the suggestion is still evident from the bifurcation diagram.

As suggested in Section 4, the bifurcation perspective can be of use in designing experiments, especially when the primary parameters can be controlled in the experiment. Models can be validated by setting up experiments in which parameter values are manipulated to cross over bifurcation curves in the parameter space. For example, our model implies that successful formation of facultative-obligate or obligate-obligate pairs requires proper parameter values for growth rates, etc. We discussed in Section 4 how lichen symbioses could be used to parameterize the model. Comparative studies of strains of cyanobacteria and fungi with genetically determined growth rates that lie to one side or another of the bifurcations displayed in Fig. 5 could also be used as a test of the model.

In conclusion, the new model for 2-dimensional mutualism proposed here appears to be a better model than either Dean's (1983) model or the logistic model with Lotka-Volterra interaction terms. This is evident in the ability of the model to describe a variety of interactions which seem ecologically logical, including the possibility of thresholds and the impossibility of unbounded growth. It is also evident in its ability to describe both facultative and obligate mutualisms and smooth transitions between these two types of mutualism.

6 Acknowledgements

The authors acknowledge useful conversations with H. W. Stech in the development and analysis of the model.

Appendix: The singularity in Dean's model

Dean (1983) introduced the following two species eight-parameter model of mutualism:

$$\frac{dx}{dt} = \frac{r_x x(k_x - x)}{k_x}$$
$$\frac{dy}{dt} = \frac{r_y y(k_y - y)}{k_y} \qquad \text{(A.1)}$$

where

$$k_x = K_{\max x}\left\{1 - e^{-\left(\frac{a_x y + C_x}{K_{\max x}}\right)}\right\}$$
$$k_y = K_{\max y}\left\{1 - e^{-\left(\frac{a_y x + C_y}{K_{\max y}}\right)}\right\}. \qquad \text{(A.2)}$$

Briefly, the problem with this model occurs when the expressions for the carrying capacity in equation (A.2) are not positive. By inspection, $k_x=0$ when $y=-C_x/a_x$ and $k_y=0$ when $x=-C_y/a_y$. The differential equation (A.1) is therefore singular along these lines in the phase space. When C_x or C_y is negative, the respective singular line passes through the first quadrant of phase space and is therefore significant in the ecological interpretation of the model. Consequently, all such figures in Dean (1983) (Figs. 2b, 2c, 3c, 4a, 4b), while ecologically correct, are at odds with model (A.1). From another point of view, all of the figures in Dean (1983) are correct if Dean's model is replaced by ours.

In Fig. 6 we illustrate with two phase space figures from Dean (1983), one for facultative-facultative mutualism (6A), and one for obligate-obligate mutualism (6B). In Fig. 6C and 6D, respectively, we redraw Fig. 6A and 6B, this time with the singularities. Since the singular lines in Fig. 6C do not enter the first quadrant, Fig. 6A is correct. The singular lines do, however, enter the first quadrant in Fig. 6D, so the phase portrait of Fig. 6B is not correct. Corresponding flow direction arrows change direction not only when nullclines are crossed but also when the singular lines are crossed. Fig. 6E shows the phase portrait with corrected flow directions for this obligate-obligate case.

Works Cited

Ahmadjian V. 1967. *The Lichen Symbiosis*. Blaisdell Publishing Co., Waltham, Mass.

Büdel, B. 1992. Taxonomy of lichenized procaryotic blue-green algae. *In* Algae and symbioses: plants, animals, fungi, viruses. Interactions explored. *Edited by* W. Reisser. Biopress Limited, Bristol. pp. 301-324.

Dean, A.M. 1983. A simple model of mutualism. Am. Nat. **121**(3):409-417.

Goh, B.S. 1979. Stability in models of mutualism. Am. Nat. **113**(2): 261-275.

Gotelli, N.J. 1998. *A Primer of Ecology*, 2nd ed., Sinauer Associates, Massachusetts.

Graves, W G 2003, "A Comparison of Some Simple Models of Mutualism," Master's Project, University of Minnesota Duluth Technical Report TR 2003-8, available from the authors by request.

Guckenheimer, J. and Holmes, P. 1983. *Nonlinear Oscillations, Dynamical Systems and Bifurcations Vector Fields*, Springer, New York.

He, X., Gopalsamy, K. 1997. Persistence, attractivity, and delay in facultative mutualism. J. Math. Anal. Appl. **215**:154-173.

Hernandez, M.J. 1998. Dynamics of transitions between population interactions: a nonlinear interaction alpha-function defined. P. Roy Soc Lond. B Bio. **265**(1404):1433-1440.

Hirsch, M.W., Smale, S., Devaney, R.L. 2004. *Differential Equations, Dynamical Systems and An Introduction to Chaos*, 2nd edition, Elsevier/Academic Press.

Kot, M. 2001. *Elements of Mathematical Ecology*. Cambridge University Press, Cambridge UK.

Miadlikowska, J., and Lutzoni, F. 2004. Phylogenetic classification of peltigeralean fungi (*Peltigerales*, *Ascomycota*) based on ribosomal RNA small and large subunits. Am. J. Bot. **91(3)**: 449-464.

Miadlikowska, J., Lutzoni, F., Goward, T., Zoller, S., and Posada, D. 2003. New approach to an old problem: incorporating signal from gap-rich regions of ITS and rDNA large subunit into phylogenetic analyses to resolve the *Peltigera canina* species complex. Mycologia **95(6)**: 1181-1203.

Nutman, P.S., editor. 1976. *Symbiotic Nitrogen Fixation in Plants*. Cambridge University Press, Cambridge, UK.

Pandey, K.D., Kashyap, A.K., and Gupta, R.K. 2000. Nitrogen-fixation by non-heterocystous cyanobacteria in an Antarctic ecosystem. Isr. J. Plant Sci. **48(4)**: 267-270.

Peckham, B.B., 1986-2006. *To Be Continued …* (Continuation Software for Discrete Dynamical Systems), http://www.d.umn.edu/~bpeckham//tbc_home.html (continually under development).

Rai, A.N. 1988. Nitrogen metabolism. *In CRC Handbook ofLichenology*. Volume 1. *Edited by* M. Galun. CRC Press, Boca Raton, Florida. pp. 201-237.

Rai, B., Freedman, H.I., Addicott, J.F. 1983. Analysis of three species models of mutualism in predator-prey and competitive systems. Math. Biosci. **65**:13-50.

Robinson, C. 2004. *An Introduction to Dynamical Systems, Continuous and Discrete,* Pearson/Prentice-Hall.

Roughgarden, J. 1998. *Primer of Ecological Theory*, Prentice Hall, New Jersey.

Sterner, R.W. and Elser, J.J. 2002. *Ecological Stoichiometry*. Princeton University Press, Princeton, NJ.

Stewart, W.D.P. 1980. Some aspects of structure and function on N_2-fixing cyanobacteria. Annu. Rev. Microbiol. **34**: 497-536.

Strogatz, S.H. 1994. *Nonlinear Dynamics and Chaos*, Perseus Books.

Vandermeer, J.H., Boucher, D.H. 1978. Varieties of mutualistic interaction in population models. J. Theor. Biol. **74**: 549-558.

Wolin, C.L. 1985. The population dynamics of mutualistic systems. In: D.H. Boucher (ed.) *The Biology of Mutualism*, Oxford University Press, New York p.248-269.

Table 1. Equilibria and associated eigenvalues for the local analysis (equivalent to the Lotka-Volterra model for mutualism).

Equilibrium label	Equilibrium	Eigenvalues
0	(0,0)	r_{10}, r_{20}
1	$\left(\frac{r_{10}}{a_1},0\right)$	$-r_{10}$, $\frac{b_2 r_{10}}{a_1}+r_{20}$
2	$\left(0,\frac{r_{20}}{a_2}\right)$	$-r_{20}$, $\frac{b_1 r_{20}}{a_2}+r_{10}$
3	$\left(\frac{a_2 r_{10}+b_1 r_{20}}{a_1 a_2-b_1 b_2},\frac{b_2 r_{10}+a_1 r_{20}}{a_1 a_2-b_1 b_2}\right)$	Complicated expression.

Table 2. Equilibria and associated eigenvalues for the global analysis (the full model proposed).

Equilibrium label	Equilibrium	Eigenvalues
0	(0,0)	r_{10}, r_{20}
1	$\left(\frac{r_{10}}{a_1},0\right)$	$-r_{10}$, ,r_{20}
2	$\left(0,\frac{r_{20}}{a_2}\right)$	r_{10}, $-r_{20}$
3	Lower left intersection of nonlinear nullclines, when an intersection exists. Location determined numerically.	Both real and negative when in the first quadrant (stable coexistence!), other stabilities in other quadrants
4	Upper right intersection of nonlinear nullclines, when an intersection exists. Location determined numerically.	One positive and one negative when in the first quadrant (threshold!), other stabilities in other quadrants

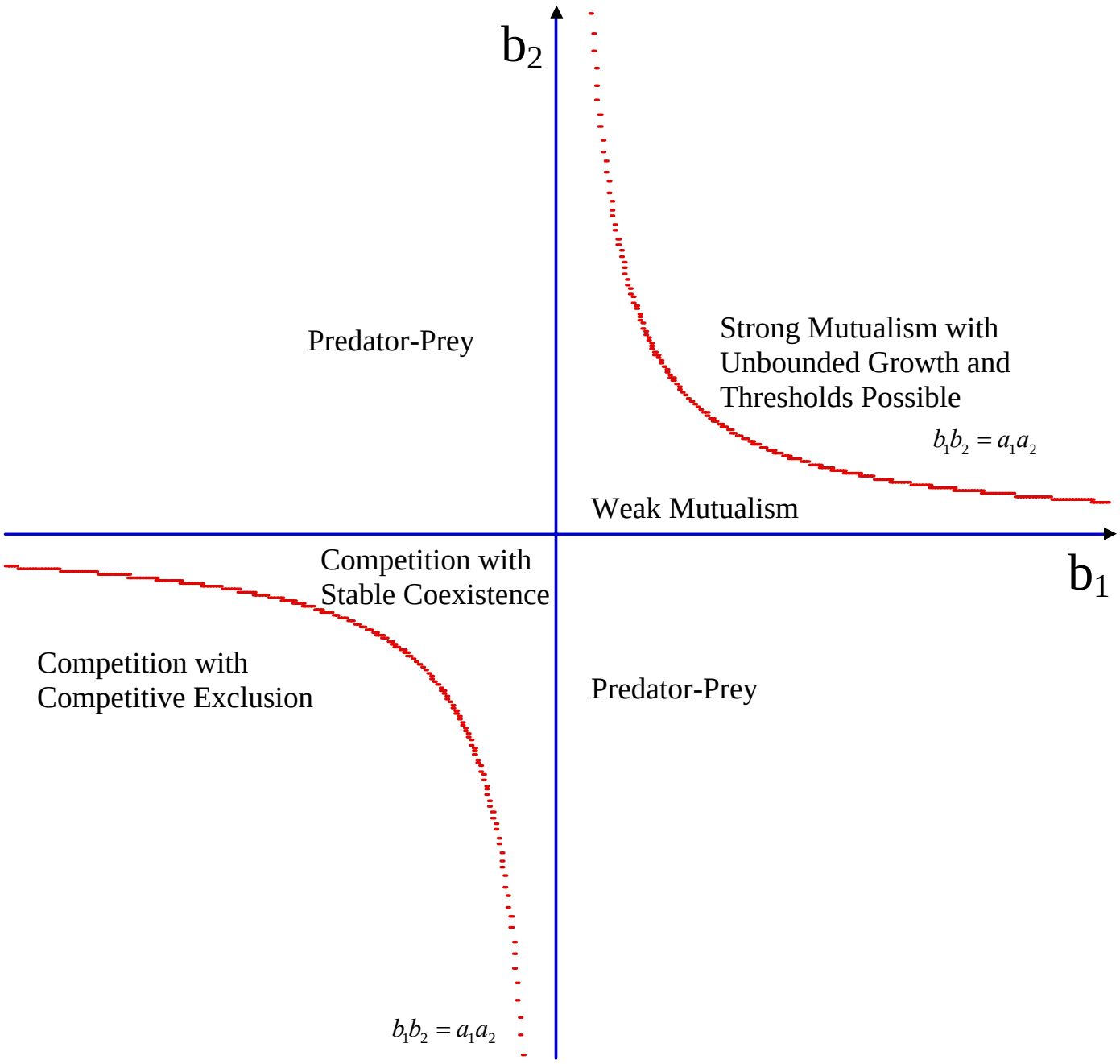

Figure 1: Lotka-Volterra interaction space: b_2 vs b_1. The curve for $b_1b_2 = a_1a_2$ appears in the first and third quadrants and is calculated with $a_1=1$ and $a_2=1$. In the first quadrant, mutualisms with coefficient Cartesian pairs that lie below/left of the curve give rise to weak ("stable") mutualisms whereas mutualisms with coefficient Cartesian pairs that lie above/right of the curve give rise to strong (unstable, with unbounded growth) mutualisms. In the third quadrant, competitive species with coefficient Cartesian pairs that lie above/right of the curve give rise to competition that need not exhibit competitive exclusion whereas competitive species with coefficient Cartesian pairs that lie below/left of the curve give rise to competition that does exhibit competitive exclusion.

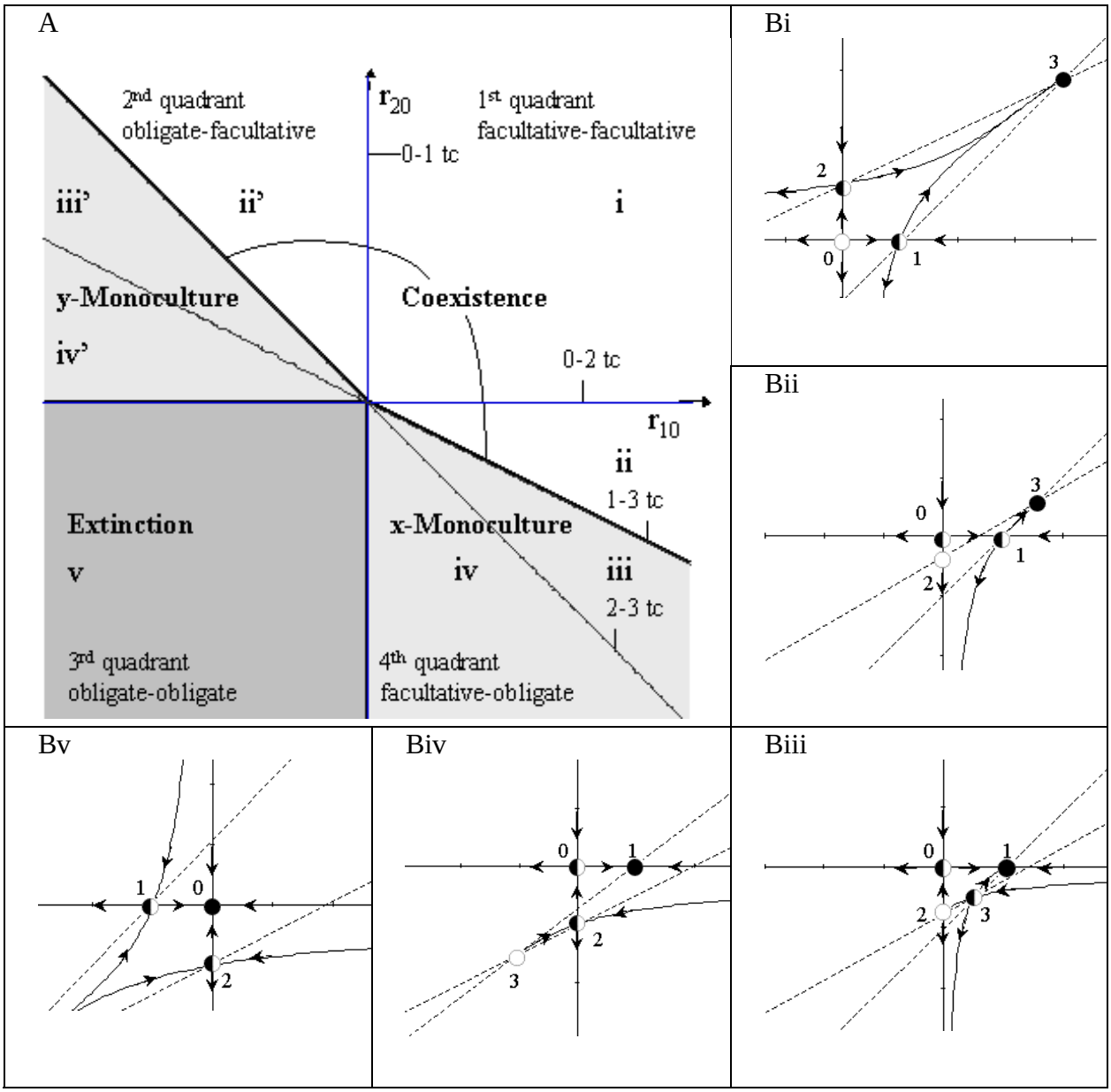

Figure 2: Weak Lotka-Volterra mutualism, ($a_1a_2 > b_2b_1$).: (A) the bifurcation diagram in r_{20} vs r_{10}. Key: thick lines ="ecologically significant," tc = transcritical; the labels of the equilibria involved in the bifurcation (see section 3.3) precede the bifurcation abbreviation. (B) representative phase portraits for the corresponding regions in (A). Dashed lines are nullclines; solid lines are stable or unstable manifolds of saddle equilibria. By interchanging x and y, similar phase portraits would result for regions labeled with primed numbers. Auxiliary parameters: $a_1 = 1$, $a_2 = 1$, $b_1 = 1$, and $b_2 = 0.5$. Primary parameters: $r_1 = 1$, $r_2 = 1$ for i; $r_1 = 1$, $r_2 = -0.25$ for ii; $r_1 = 1$, $r_2 = -0.75$ for iii; $r_1 = 0.5$, $r_2 = -1$ for iv; and $r_1 = -1$, $r_2 = -1$ for v.

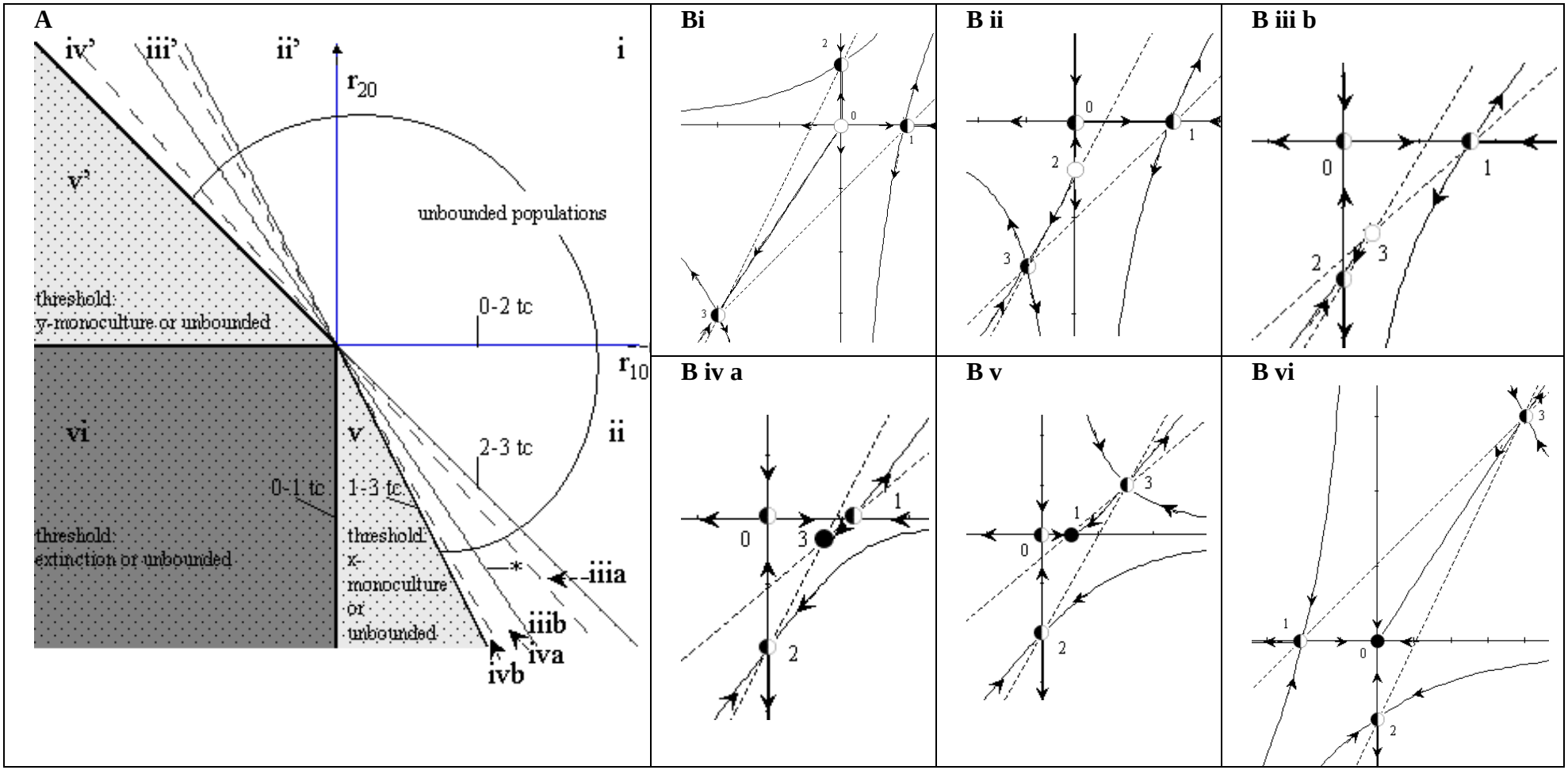

Figure 3: Strong Lotka-Volterra mutualism ($a_1a_2 < b_1b_2$). (A) bifurcation diagram in r_{20} vs r_{10}. Thick lines are "ecologically significant." The dashed lines are parameter values where the eigenvalues of the co-existence equilibrium are equal. Key: tc=transcritical, *=double bifurcation curve (Hopf and heteroclinic), dashed lines=equal eigenvalues for the corresponding equilibrium, thick line="ecologically significant," dotted background = region with threshold behavior. Equilibrium labels are in Section 3.3. (B) representative phase portraits for corresponding regions in (A). Auxiliary parameters: $a_1 = a_2 = 1$, $b_1 = 1$, and $b_2 = 2$; primary parameters: $r_{10} = 1.0$, $r_{20} = 1.0$ for i; $r_{10} = 1.0$, $r_{20} = -0.5$ for ii; $r_{10} = 0.833$, $r_{20} = -1.0$ for iii b; $r_{10} = 0.583$, $r_{20} = -1.0$ for iv a; $r_{10} = 0.25$, $r_{20} = -1.0$ for v; and $r_{10} = -1.0$, $r_{20} = -1.0$ for vi.

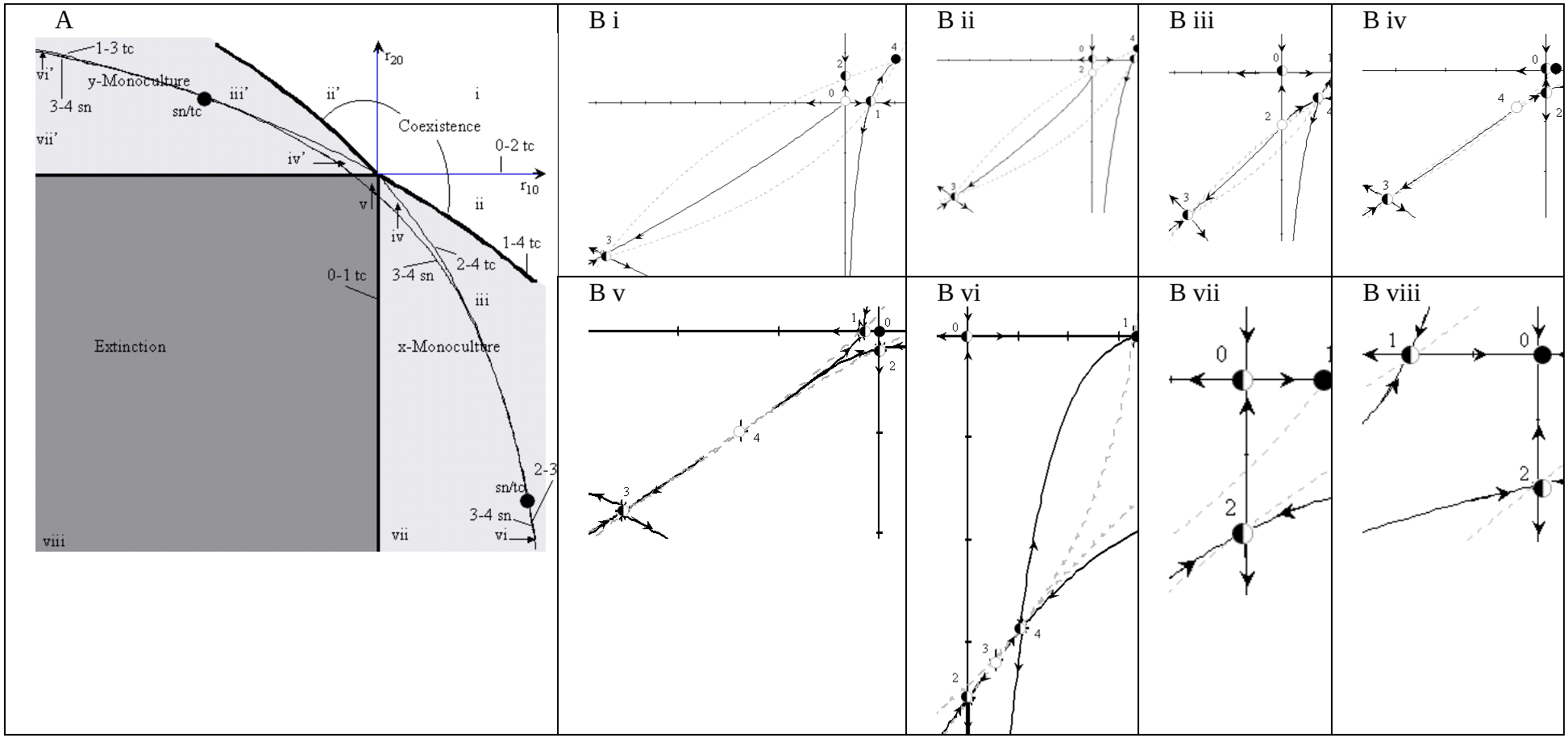

Figure 4: Full mutualism model, locally weak case. (A) Bifurcation diagram in: r_{20} vs r_{10}. Key: thick lines = "ecologically significant," tc=transcritical, sn=saddle-node, sn/tc=point of tangency between saddle-node and transcritical curves. Note that the equilibrium pairings on the tc curves change when passing through the tc/sn tangency. Equilibrium labels are in Section 3.3. (B) Representative phase portraits. Auxiliary parameters: $a_1 = 1$, $a_2 = 1$, $k_1 = 0.5$, $k_2 = 0.25$ $r_{11} = 2$, and $r_{21} = 2$; primary parameters: $r_{10} = 0.5$, $r_{20} = 0.5$ for i; $r_{10} = 1$, $r_{20} = -0.3$ for ii; $r_{10} = 1$, $r_{20} = -1$ for iii; $r_{10} = 0.1$, $r_{20} = -0.2$ for iv; $r_{10} = -0.1$, $r_{20} = -0.1$ for v; $r_{10} = 1.65$, $r_{20} = -3.56$ for vi; $r_{10} = 0.5$, $r_{20} = -1$ for vii; $r_{10} = -1$, $r_{20} = -1$ for viii.

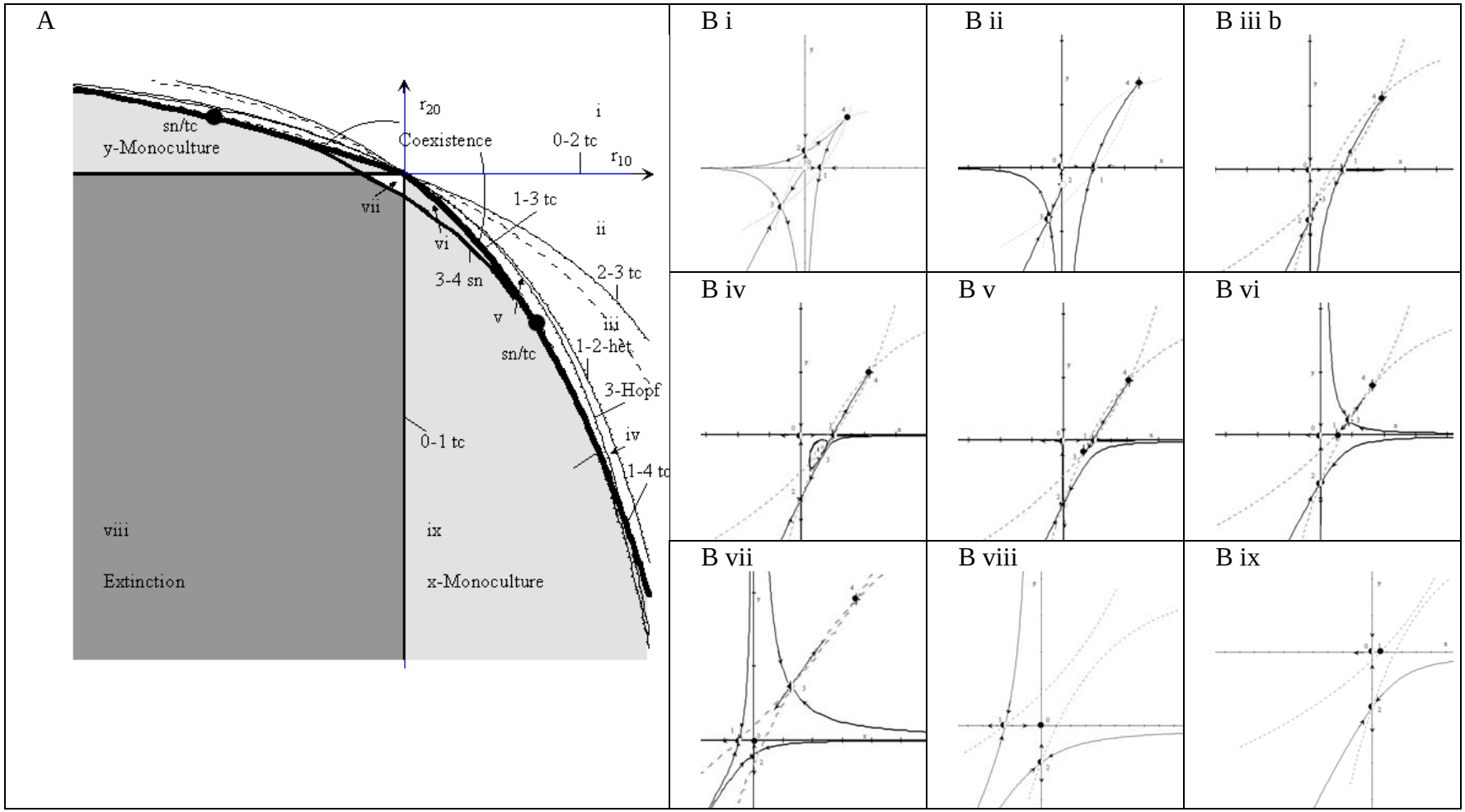

Figure 5: Full mutualism model, locally strong case. (A) bifurcation diagram in: r_{20} vs r_{10}. Key: thick lines = "ecologically significant," dashed lines = curves along which the corresponding equilibrium has equal eigenvalues, tc=transcritical, sn=saddle-node, het=heteroclinic connection, sn/tc=point of tangency between saddle-node and transcritical curves. Equilibrium labels are in Section 3.3.2. Auxiliary parameters: $a_1 = 1$, $a_2 = 1$, $k_1 = 0.5$, $k_2 = 1$, $r_{11} = 2$, and $r_{21} = 2$; primary parameters: $r_{10} = 0.5$, $r_{20} = 0.5$ for i; $r_{10} = 0.5$, $r_{20} = -0.25$ for ii; $r_{10} = 0.5$, $r_{20} = -0.75$ for iii b; $r_{10} = 0.5$, $r_{20} = -0.995$ for iv; $r_{10} = 0.46$, $r_{20} = -1$ for v; $r_{10} = 0.25$, $r_{20} = -0.75$ for vi; $r_{10} = -0.1$, $r_{20} = -0.1$ for vii; $r_{10} = -0.5$, $r_{20} = -0.5$ for viii; $r_{10} = 0.1$, $r_{20} = -0.75$ for ix.

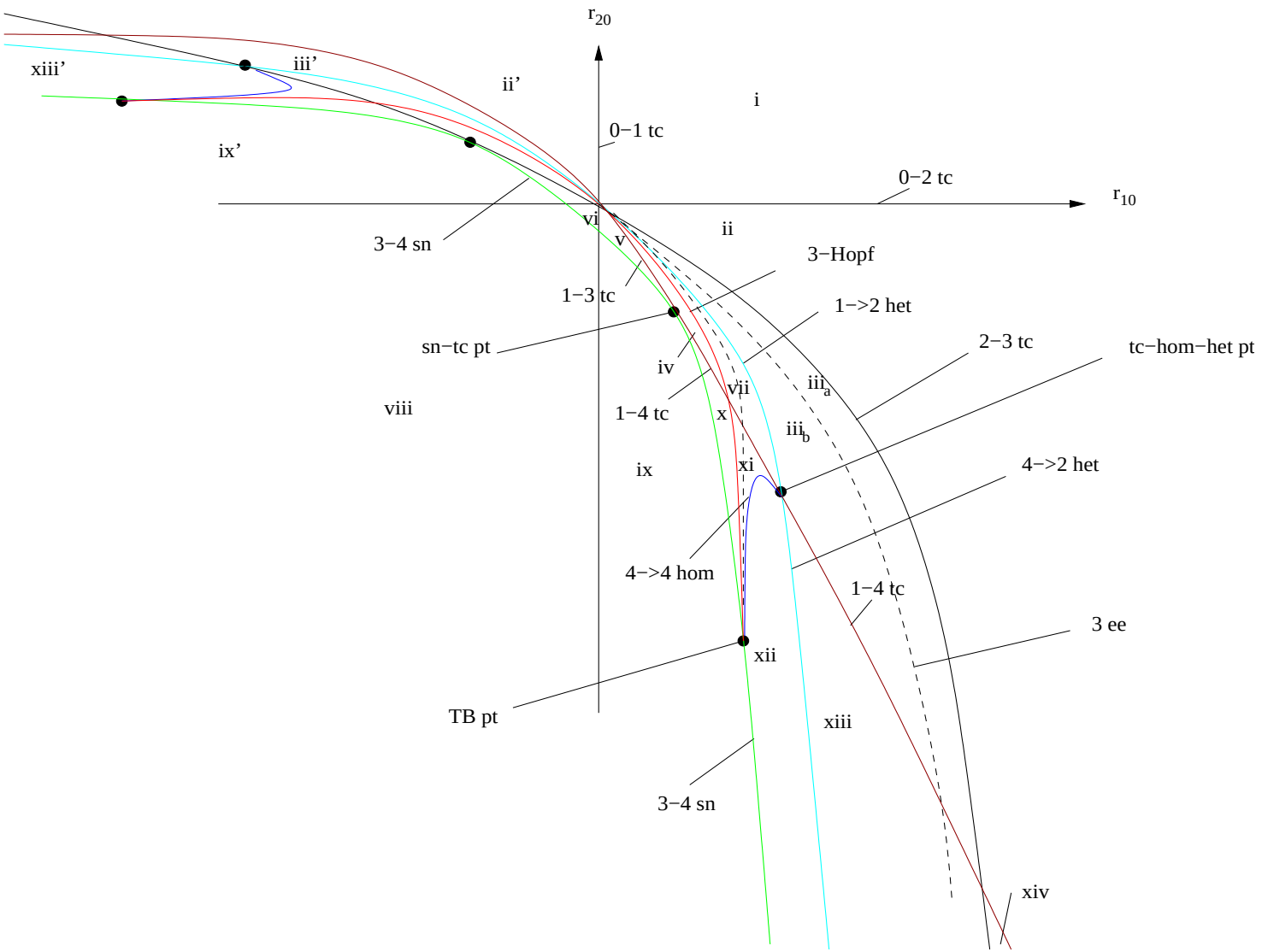

Fig 5A schematic. Corresponding igure 5B schematics next three pages.

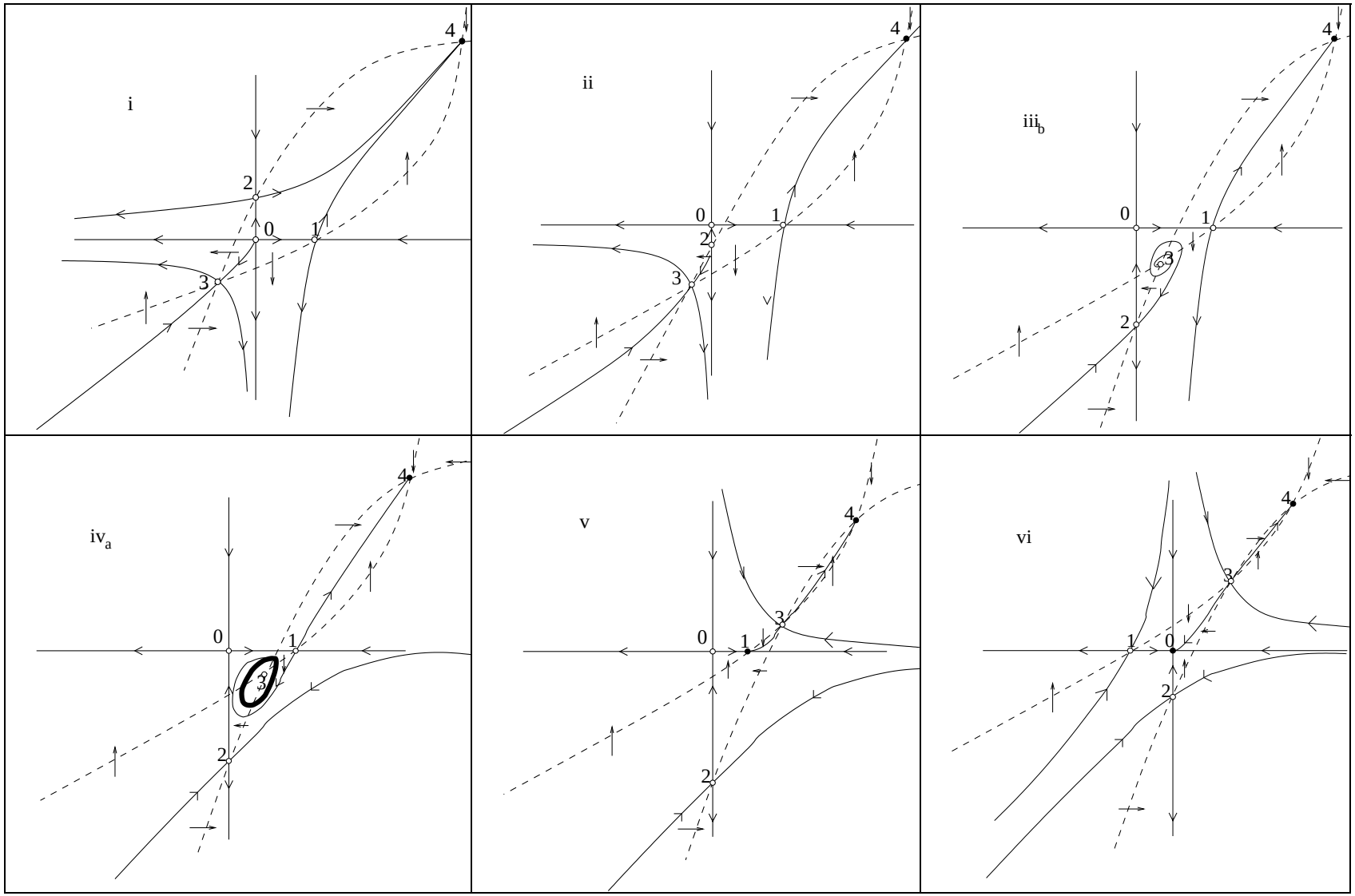
i
ii
iii$_b$
iv$_a$
v
vi
0
1
2
3
4

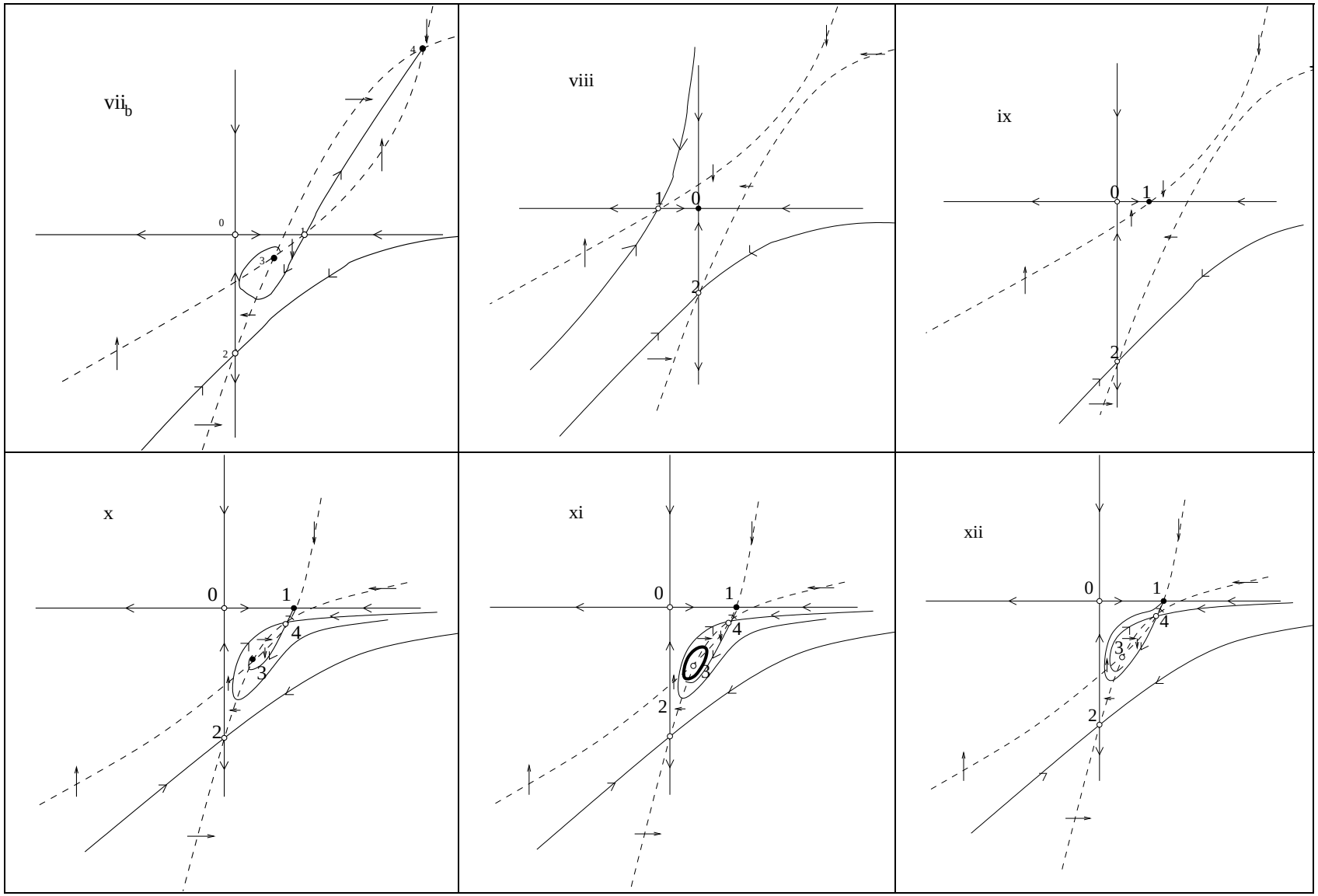
vii$_b$
0
1
2
3
4
viii
1
0
2
ix
0
1
2
x
0
1
2
3
4
xi
0
1
2
3
4
xii
0
1
2
3
4

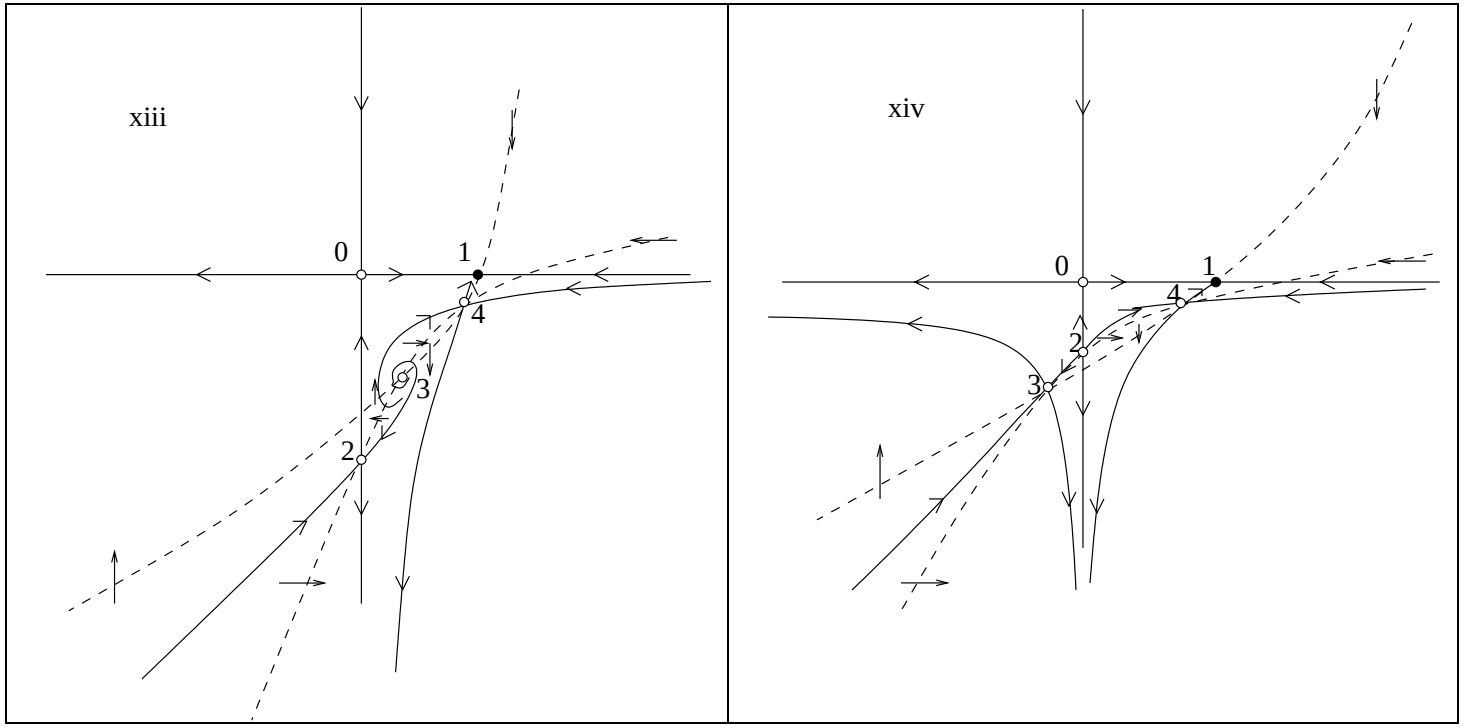
xiii
0
1
4
3
2
xiv
0
1
4
2
3

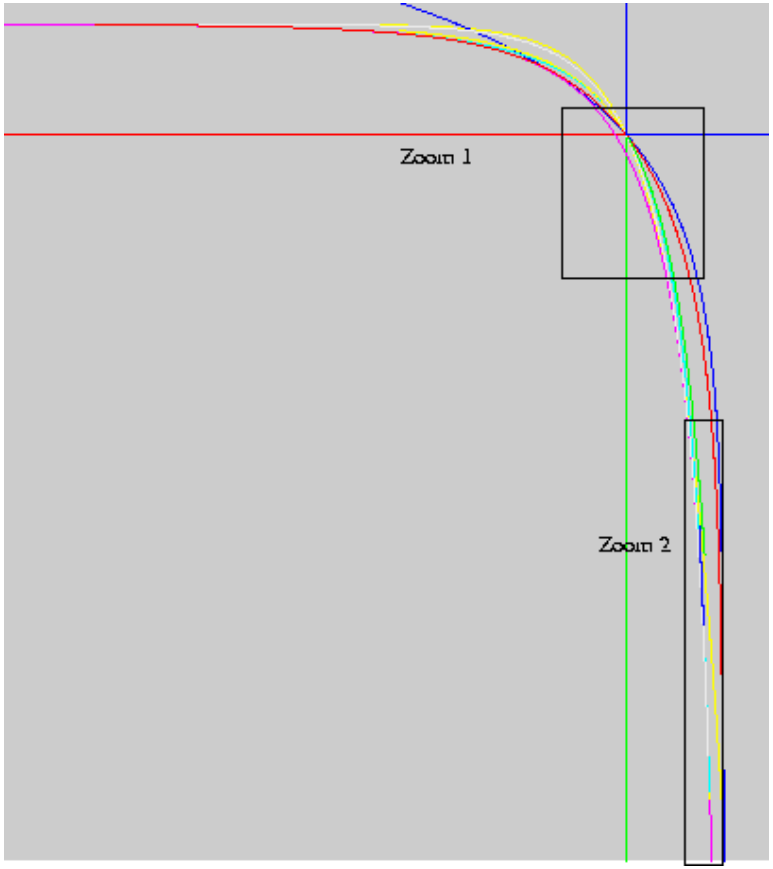

Figure 5A numerically computed with TBC.

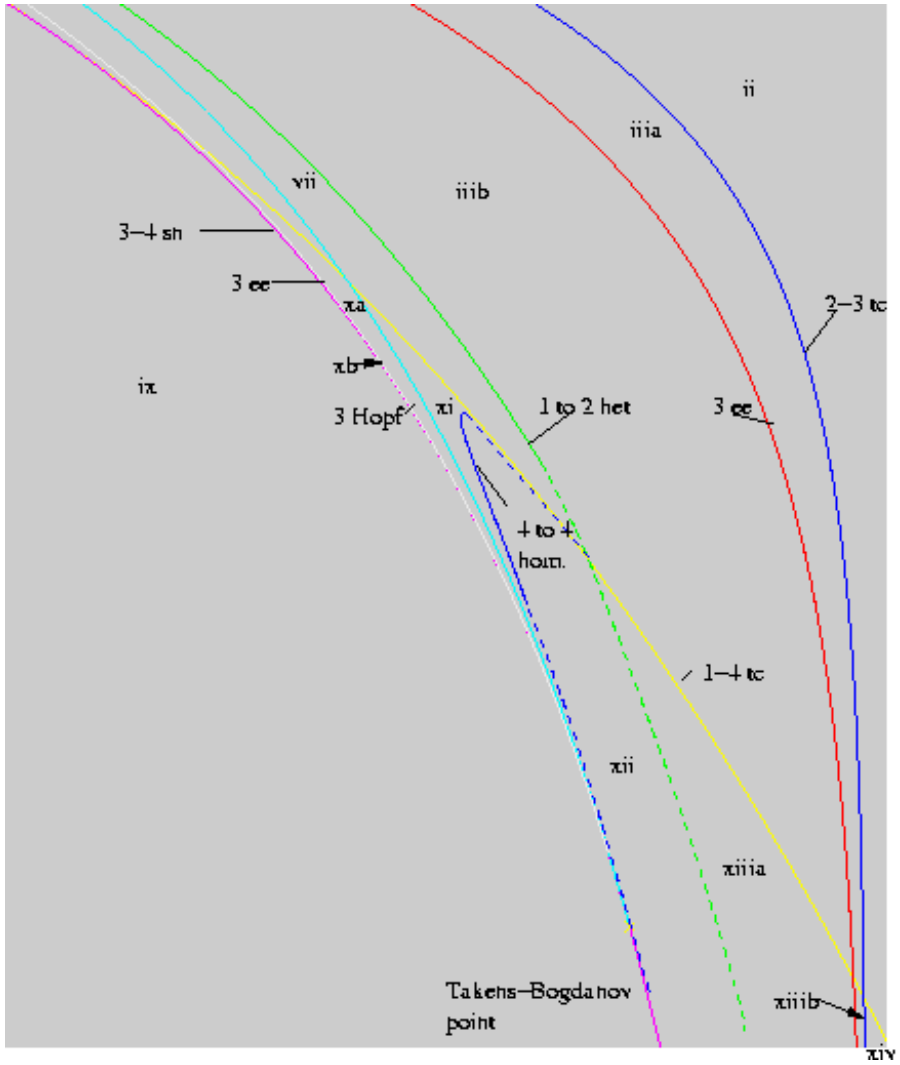
ii
iiia
iiib
vii
3–+ sh
3 ee
xa
xb
ix
3 Hopf
xi
1 to 2 het
3 ee
2–3 tc
+ to +
horn.
1–+ tc
xii
xiiia
Takens–Bogdanov
point
xiiib
xiv

Fig. 5A, Zoom 2.

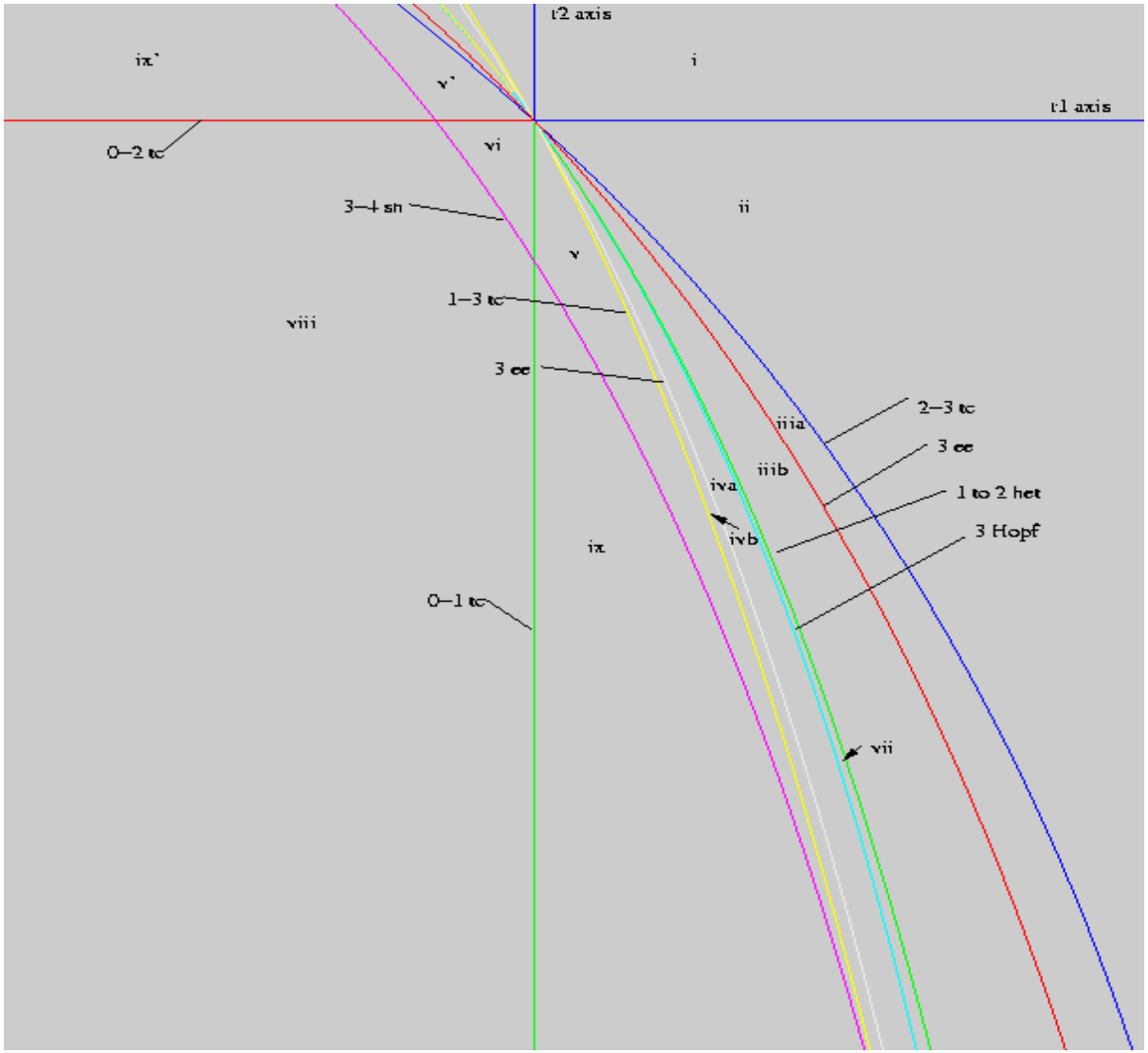
t2 axis
t1 axis
i
ii
iii
iiia
iiib
iv
iva
ivb
v
v'
vi
vii
viii
ix
ix'
0–2 tc
3–4 sn
1–3 tc
3 ee
0–1 tc
2–3 tc
3 ee
1 to 2 het
3 Hopf
Fig 5A, zoom 1.

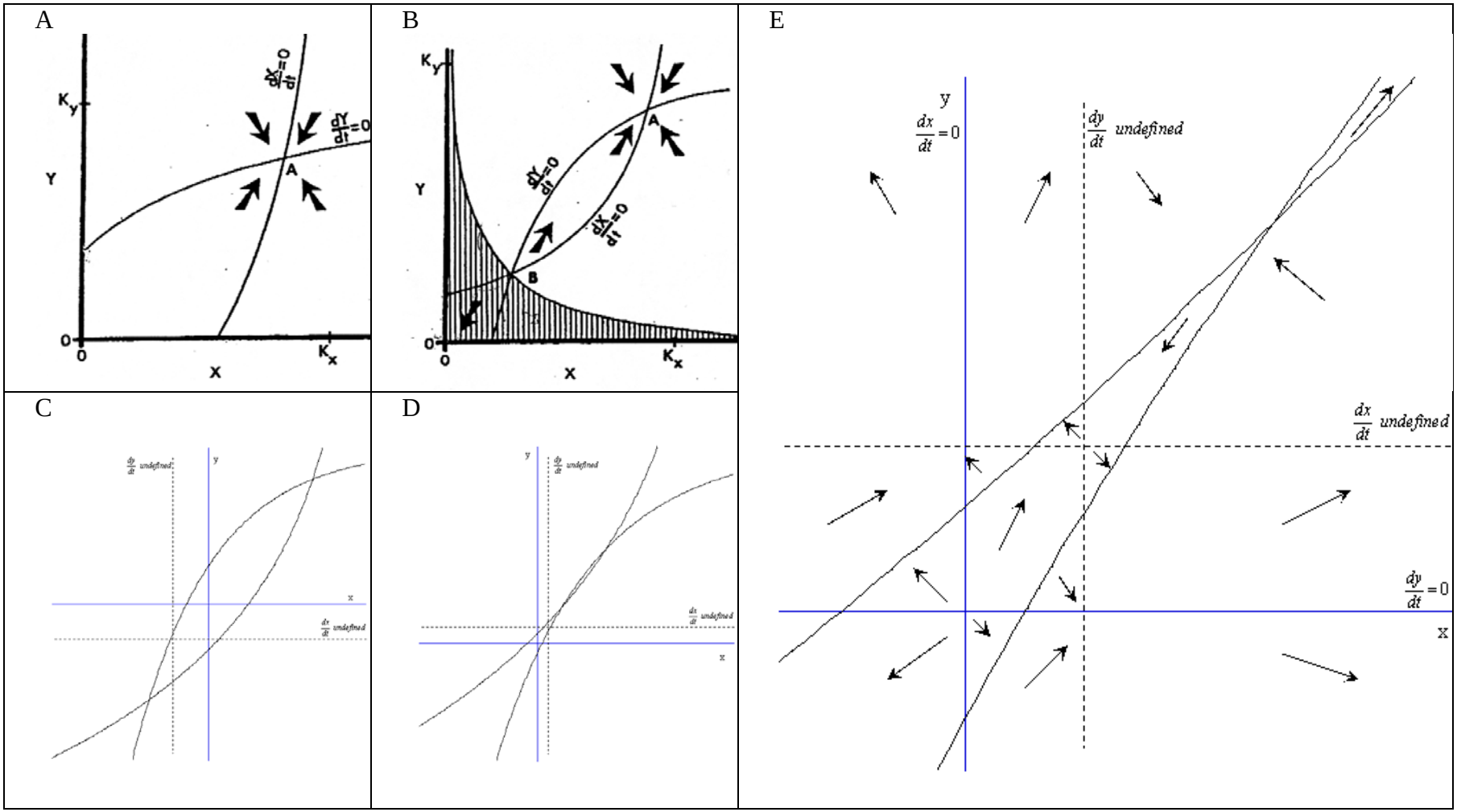

Figure 6: Singularities in the Dean (1983) phase portraits. (A) Dean's figure 3a, facultative-facultative case, first quadrant only; (B) Dean's figure 3b, obligate-obligate case, without singularities marked; (C) extension of (A) to include singularities (dashed lines) in quadrants 2, 3, and 4; (D) extension of (B) to include singularities; (E) enlargement of the region near the origin in (D) ; arrows indicate corrected flow directions; flow directions change on either side of nullclines AND on either side of the discontinuities.